ACI STRUCTURAL JOURNAL TECHNICAL PAPER

Title no. 87-S18

Tests of Post-Tensioned Concrete Slab-Edge Column Connections

by Douglas A. Foutch, William L. Gamble, and Harianto Sunidja

The results of tests of four connections between reinforced concrete exterior columns and post-tensioned slabs are presented. The specimens, at about two-thirds scale, had steel arrangements representative of banded-tendon layouts, and two specimens had many closely spaced tendons while the other two had only a few widely spaced tendons. The connections also contained reinforcing bars typical of those normally used in these cases. Bending and shear forces were applied to cause failure. Both primary bending failures and primary shear failures occurred.

The current ACI Building Code (ACI 318-83) recognizes that the precompression in the concrete, expressed as f_{pc}, enhances the shear strength of an interior column-slab connection. The present series of tests indicates that the same benefit of precompression can safely be extended to the edge column-slab connection case. The ACI Building Code places an upper limit of f_{pc} = 500 lb/in.^{2} (3.45 MPa) on the precompression that can be utilized in the shear calculation. Two of the specimens in these tests had f_{pc} values considerably higher than this limit, which does not appear to be necessary.

The ACI Building Code also limits the useful compressive strength of concrete to f'_c = 500 lb/in.^{2} (34.5 MPa) for purposes of shear-strength calculations. This limit does not appear to be necessary, since the concrete strengths in these test specimens were considerably higher, and the shear strength prediction equations remained valid.

Keywords: columns (supports); concrete slabs; connections; flat concrete slabs; flexural strength; **post-tensioning;** prestressed concrete; reinforced concrete; shear strength; **tests.**

Prestressed flat-plate floor construction is widely used for commercial and residential construction in many parts of the United States. This system is very economical because of the simple formwork, minimum floor-to-floor height, and minimum obstruction to utility and duct placement. It also results in aesthetically pleasing lines and good fire-resistance properties.

The majority of prestressed flat plates are constructed using unbonded post-tensioned tendons because of speed of construction and other economic considerations. The use of a banded-tendon arrangement to simplify construction has become popular, even though this differs from ACI Building Code[1,2] recommendations. The tendons in this type of construction are grouped in a narrow band over the column line in one direction, while the tendons in the orthogonal direction are uniformly distributed. Fig. 1 shows the typical layout of the banded-tendon layout of a two-thirds scale model slab.

Although the study of ordinary slab-column connections has received considerable attention, uncertainties still exist concerning the response of prestressed slabs, even when this structural system is loaded statically. One of the major problems lies in the connections between the slab and its supporting columns. Large bend-

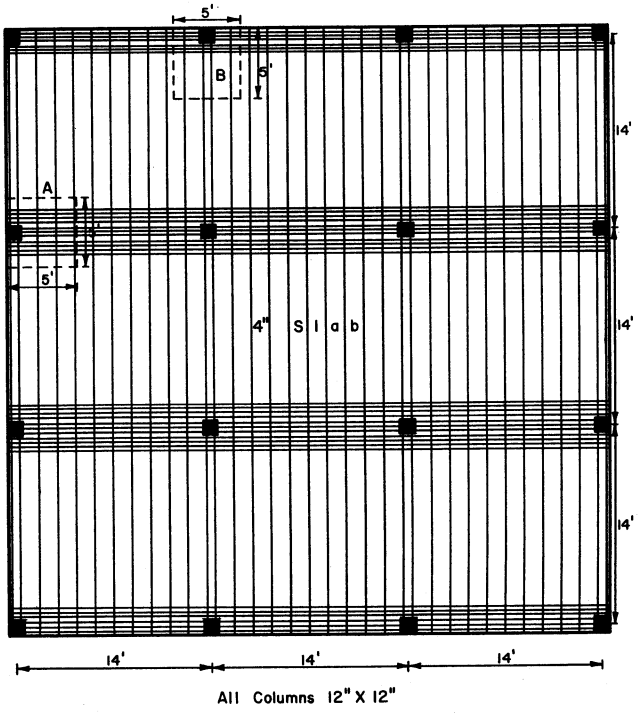

Fig. 1—Two-thirds scale model of prestressed concrete slab

ACI Structural Journal, V. 87, No. 2, March-April 1990.

Douglas A. Foutch is Professor of Civil Engineering at the University of Illinois at Urbana, where he is engaged in teaching and research in structural engineering. He has specialized in dynamic analysis problems related to seismic and wind loadings.

William L. Gamble, FACI, is Professor of Civil Engineering at the University of Illinois at Urbana, where he is engaged in teaching and research in the fields of prestressed and reinforced concrete structures. He is Chairman of ACI Committee 216, Fire Resistance and Fire Protection of Structures, and is a member of ACI Committee 543, Concrete Piles, and of joint ACI-ASCE Committees 421, Design of Reinforced Concrete Slabs, and 423, Prestressed Concrete.

Harianto Sunidja is presently Associate Dean for Academic Affairs, Department of Engineering, University of Indonesia, Jakarta, Indonesia. He received his PhD in Civil Engineering from the University of Illinois at Urbana in 1982. He also serves as Deputy Director of VSL Indonesia.

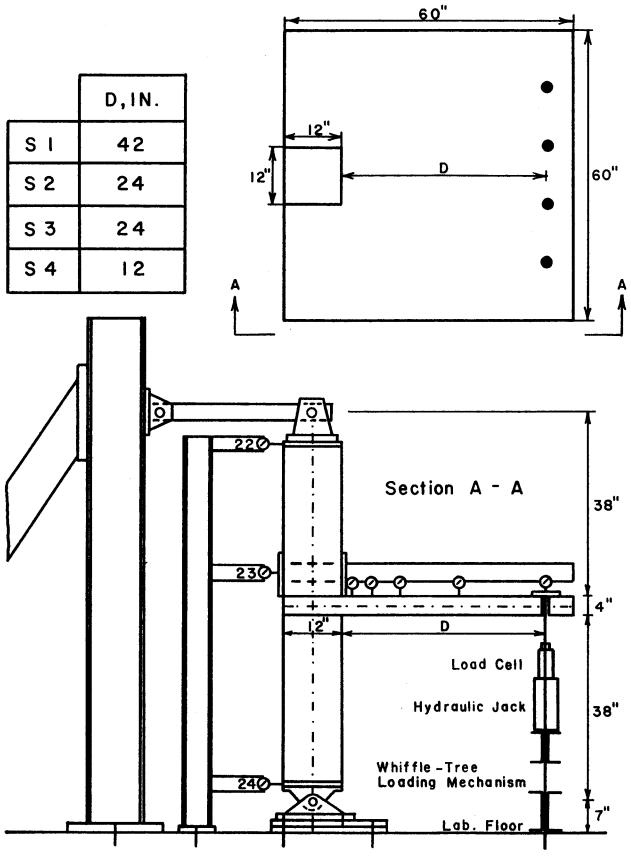

Fig. 2—Plan and elevation of the test specimen

ing moments as well as shear forces are concentrated at the connection, so the connection is susceptible to punching-shear failure. For edge columns in particular, the presence of the free edge adds further to the concentrated stress condition at the connection. The complexity of the three-dimensional stress distribution in the plate immediately adjacent to a column, and the large number of interdependent parameters involved, have precluded the development of a general analytical solution for calculating the strength of these connections. The methods commonly used for design employ either approximate theoretical solutions that utilize experimentally determined constants or purely empirical expressions that satisfy experimental results.

RESEARCH SIGNIFICANCE

These tests are among the first conducted on isolated connections between post-tensioned flat-plate structures and edge columns. The design of these connections is currently based on information from tests on reinforced concrete slab-column connections, and the potential benefits of post-tensioning have been ignored because of the lack of test data. These tests provide some data on the connection strength and behavior, and they also provide some data that justify easing current limits on maximum usable concrete strength and maximum usable precompression in the concrete.

SCOPE AND OBJECTIVES

In a typical slab carrying gravity loads, shear and unbalanced moment will be present at the edge-column connections. The transfer of unbalanced bending moment causes the distribution of shear stress in the slab around the column to become nonuniform and reduces the shear strength of the connection. The main objective of this investigation was to study experimentally under static loading the strength and behavior of prestressed slab-edge column connections with unbonded tendons representative of those used in typical buildings.

Four two-thirds scale slab-edge columns were constructed and subjected to loadings in which both the shear and moment transferred between the slab and the column were increased proportionally until failure occurred. The experimental variables considered in the study were the direction of the banded tendons and the moment-shear ratio. The specific objectives of the investigation were: 1) to study the effect of moment-to-shear ratio on the response of the connection; 2) to study the increase in stress in the unbonded tendons at ultimate load; 3) to study the mechanism of failure in the connections; and 4) to develop a simple design procedure for predicting the strength of the connection. Many details beyond those in this paper are contained in Reference 3.

TEST SPECIMENS AND PROCEDURES

General description

The connection specimens tested in this program were based on the design of a two-thirds scale model of a prototype structure. The layout of the model is shown in Fig. 1. The model structure required eleven ⅜ in. (9.5 mm) diameter tendons per bay and an average prestress of about 240 psi (1.65 MPa). The test specimens were models of the edge column connections and the adjacent slab area, as indicated by the dashed lines in Fig. 1.

Since the predicted flexural strength of a slab is usually a function of the number of tendons in a particular direction and is not strongly influenced by their distribution, all tendons are usually grouped together in a narrow band in one direction over the column line, while the tendons in the orthogonal direction are uniformly distributed across the slab. The design concept is that the closely spaced tendons are thought of as

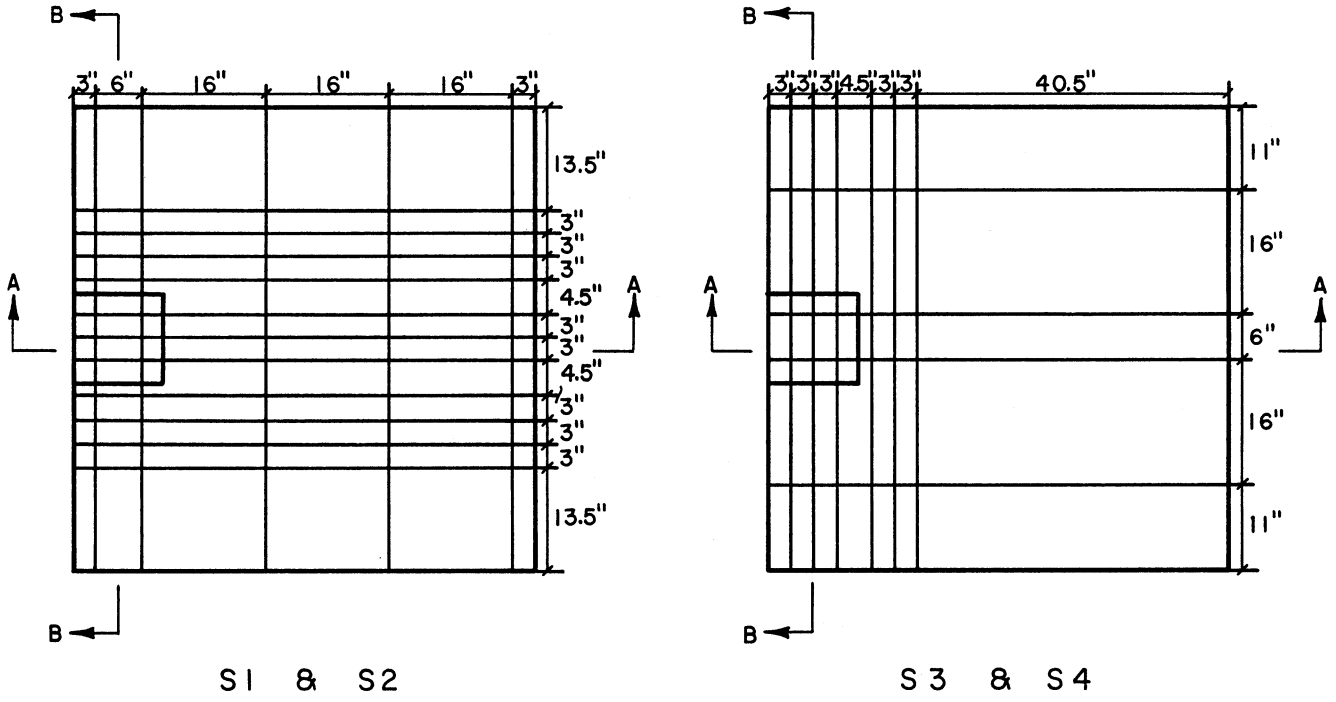

Fig. 3—Tendon arrangement

forming beams in one direction, while the slab then acts as a one-way slab in the other direction. This arrangement is common in practice because it simplifies the placing and jacking of the tendons.

Four specimens were constructed and tested. These will be referred to as Specimens S1 through S4. In the first two specimens, S1 and S2, the banded tendons were perpendicular to the exterior edge of the slab, as represented by Detail A in Fig. 1. In the other two specimens, S3 and S4, the banded tendons were parallel to the exterior edge of the slab, as represented by Detail B in Fig. 1. The effect of moment-shear ratio was investigated by applying the load at different distances from the column face.

Description of specimens

Plan and elevation views of the specimens and loading apparatus are shown in Fig. 2. Each slab consisted of a 60 in. (1524 mm) square prestressed concrete slab 4 in. (102 mm) thick, and a 12 in. (305 mm) square column located adjacent to and centered along the edge of the slab. Thus, the geometry of each specimen was identical. Plan and elevation views of the specimens showing the tendon arrangements are given in Fig. 3 and 4. In addition, No. 3 (9.5 mm) deformed bars were used as bonded reinforcement in the vicinity of the column for crack control as recommended by ACI-ASCE Committee 423.[4] No. 3 (9.5 mm) bars were also placed top and bottom around the perimeter of the slab to control cracking and splitting from anchorage forces. The layout of deformed bars is shown in Fig. 5.

The conditions at the boundary of a model should ideally be identical to those at the corresponding location in the structure being modeled. These boundary conditions cannot be satisfied exactly without testing the entire structure. The locations and shapes of contraflecture lines are not constant in a prestressed concrete system. Cracking of the slab causes the relative stiffnesses of various sections and directions to change. Redistribution of moments can and does take place in the slab, causing the location of contraflecture lines to shift. Reproducing these conditions for isolated connections is probably impossible, so the effects of continuity are not included in the present investigation.

The main reason to use isolated connection models is simplicity and ease of testing relative to the complex and expensive multipanel models. The interaction of internal actions around the connections is complex even for an elastic plate, but the complexities are confined to a localized portion of the slab in the vicinity of the column. The stress concentrations in this region are very high but decrease rapidly with distance from the column. Thus, the strengths observed in these specimens are believed to approximate closely the strengths of connections in an actual slab system. Another distinct advantage of testing isolated connection specimens is that the system is statically determinate, so that moments and shears carried by the connection may be measured directly.

Material properties

The concrete for all specimens was made from Type I portland cement, river sand, and ¾ in. (19 mm) maximum size gravel. Measured slumps ranged from 1 to 1¾ in. (25 to 44 mm) for Specimens S1 and S2, and from 2 to 2 ¾ in. (51 to 70 mm) for S3 and S4. Three

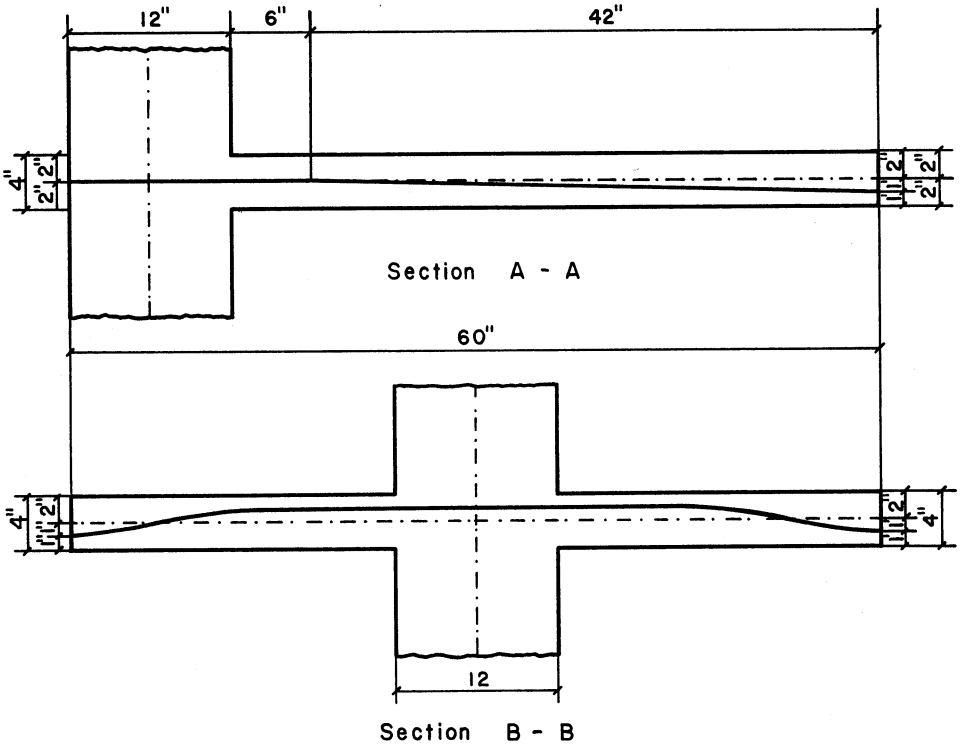

Fig. 4—Tendon profile

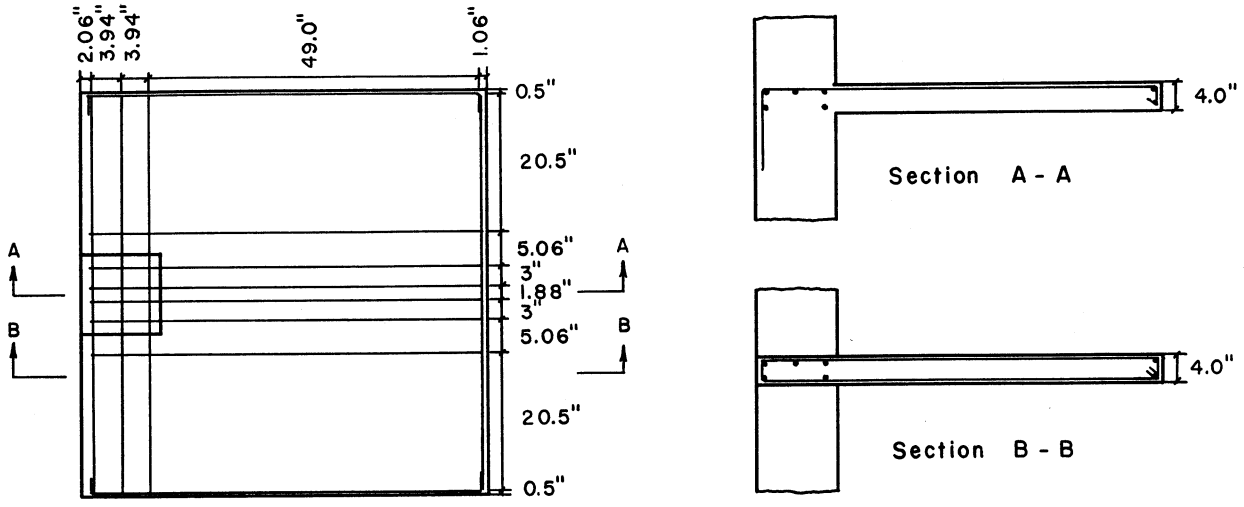

Fig. 5—Bonded reinforcement in the slab

6 by 12-in. (150 by 300-mm) cylinders were tested on the day the tendons were tensioned, and three were tested on the day of testing. In addition, three split-cylinder tension tests were carried out on 6 by 6-in. (150 by 150-mm) cylinders, and flexural beam tests were carried out on three 6 by 6 by 20-in. (150 by 150 by 500-mm) beams on the day of testing. The average measured material properties are given in Table 1.

The tendons used in the program were ⅜ in. (9.5 mm) diameter, 7-wire strands meeting the requirements of ASTM A 416. The specified minimum ultimate strength was 270 ksi (1861 MPa), and the average apparent modulus of elasticity was 28,300 ksi (195 GPa). The tendons were inserted into ½ in. (12.7 mm) diameter polyethylene tubing to prevent bonding to the concrete. All bonded bars were Grade 60 (414 MPa) with a measured average yield strength of 72.7 ksi (501 MPa) and average ultimate strength of 126.7 ksi (874 MPa).

Reusable strand chucks were used as end anchorages on the strands. For this system, the anchorage is devel-

oped by gripping the tendons with frictional-type split-cone wedges. The jacking-end grips were threaded externally and installed with nuts. In this manner, the pull-in of the wedges into the grips could be overcome by tightening the nuts against a bearing plate located between the specimen and the chuck. To provide a safety margin, the maximum recommended jacking force used was 18,400 lb (81.8 kN), whereas the ultimate strand force was 22,950 lb (102.1 kN). The strands were stressed to 16,000 lb (71.2 kN) force.

Prestressing

The slabs were post-tensioned when they were about 1 week old. The tendons were prestressed individually using a 30-ton (270 kN) hydraulic jack, which was placed between the prestressing yoke and an anchorage plate, as shown in Fig. 6. Prestressing forces were measured with aluminum sleeve load cells, which were placed between the anchorage plates and the end grips, at the anchorage ends of the strands. At the time of stressing, one load cell was also placed at the jacking end so that friction losses could be determined. However, the losses were found to be insignificant.

Since the slabs were relatively short, the losses accompanying transfer of the post-tensioning force from the hydraulic jack to the tendon were important and had to be minimized by special procedures. A tendon was initially prestressed to the desired level and then released to set the wedge-type anchor grips at each end of the tendon. The tendon was then retensioned to 16 kips (71.2 kN), the nut on the outside of the grip was screwed down against the bearing plate, and then the jack force was released. The last step was repeated several times to overcome the problem of slip at the grips to insure that the prestressing force was correct after release of the jack. The number of tendons in each direction and the average prestress for each specimen are given in Table 2.

Table 1 — Properties of concrete

Parameter	Specimen S1	S2	S3	S4
Mix by weight	1:2.98:2.78	1:2.98:2.78	1:2.98:2.78	1:2.98:2.78
w/c by weight	0.576	0.576	0.598	0.598
Slump, in.	1¼	1⅞	2	2½
At time of stressing				
Age, days	8	7	7	7
Compressive strength f'_c, psi	4700	5300	4600	4900
At time of testing				
Age, days	33	24	47	28
Compressive strength f'_c, psi	7300	6200	6100	7000
Tensile strength f_{sp}, psi	528	561	493	400
Modulus of rupture f_r, psi	726	627	702	628

1 psi = 6.895 kN/m²; 1 in. = 25.4 mm.

Table 2 — Dimensions and details of specimens

Specimen	Cross section $b \times h$, in.²	Number of ⅜ in. tendons W-E direction	N-S direction	F_{se}/A specimen, ksi W-E direction	N-S direction
S1	60 × 4	11	5	0.650	0.246
S2	60 × 4	11	5	0.691	0.325
S3	60 × 4	4	6	0.260	0.385
S4	60 × 4	4	6	0.264	0.368

1 ksi = 6.895 MPa.

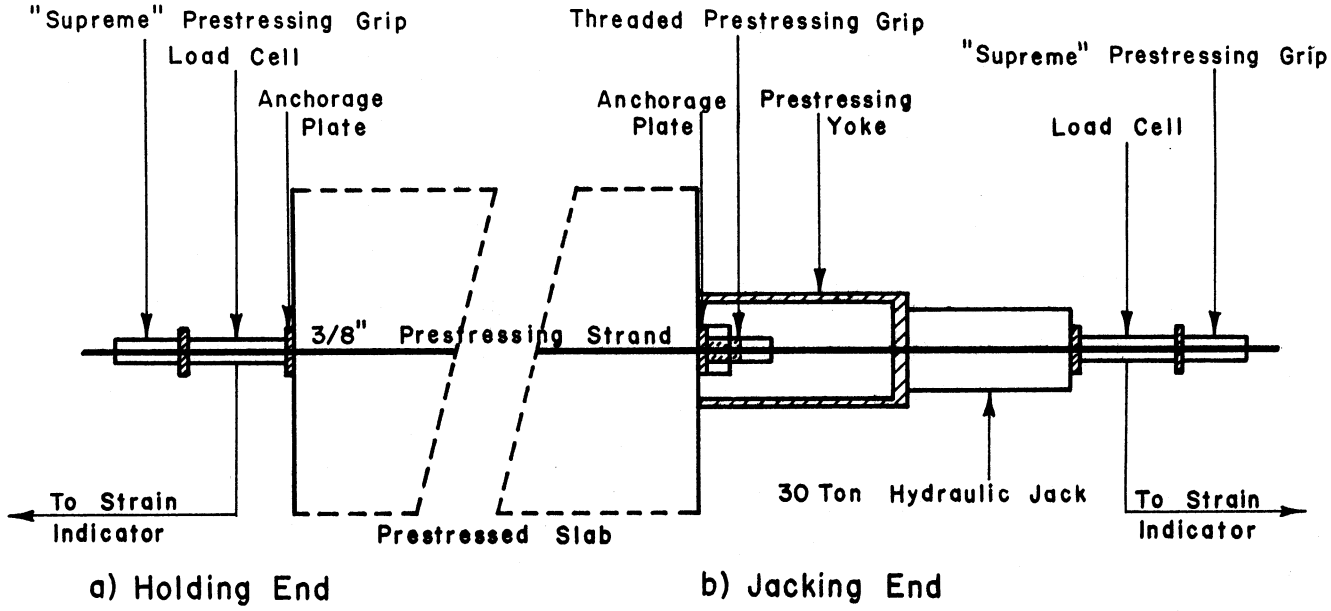

Fig. 6—Post-tensioning setup

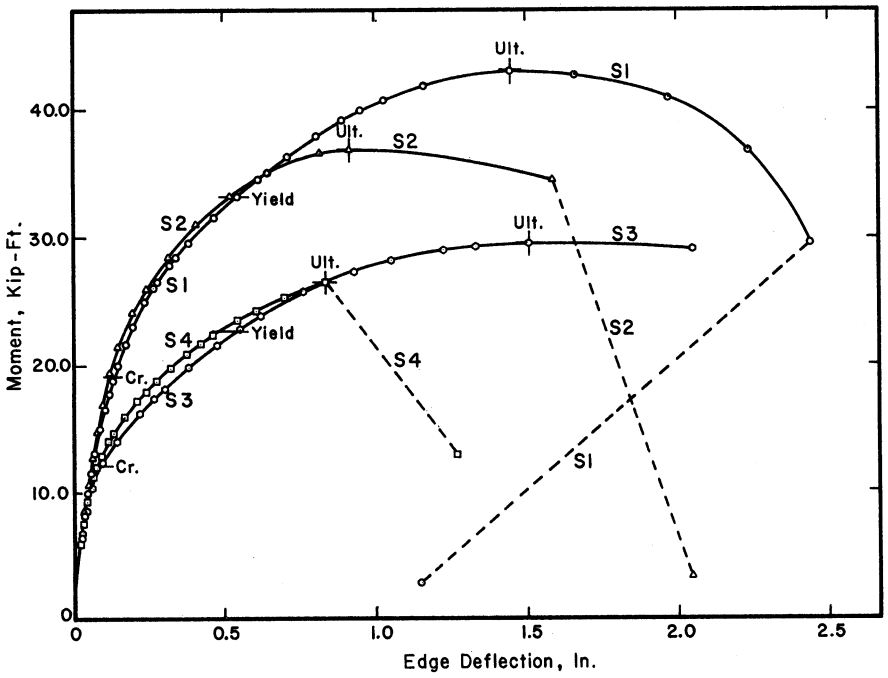

Fig. 7—Moment-deflection relationships for all specimens

Test setup and procedures

The test frame with a specimen in position is shown in Fig. 2. The unbalanced moment transferred from the slab to the column was obtained by applying a downward load to the slab through the use of two 30 ton (270 kN) hydraulic jacks and a whiffletree loading mechanism. The load was applied at four points, approximating a line load. The moment-to-shear ratio was varied from specimen to specimen by changing the distance from the face of the column at which the load was applied. The location of the loading point for each specimen is shown in Fig. 2.

During testing the deflection was held constant at the end of each load increment while the data on deflections, jack forces, prestress forces in the tendons, and strains in the bonded steel and cracks were recorded. The magnitude of the load increment was reduced near failure. The test of Slab S1 took about 12 hr, and each of the other specimens required about 7 hr to complete the test.

Each specimen was instrumented to provide detailed data on its behavior throughout the loading history. The loading forces and tendon forces were measured using aluminum sleeve load cells. Vertical deflections were measured along the east-west centerline using five mechanical dial gages, and the twisting angles of the slab were measured by eight dial gages on each side of the slab. Strain gages were used at selected locations on the surface of the slab and on the bonded top reinforcement.

TEST RESULTS

General behavior

The four specimens were each loaded by increments, and the moment at each load step was obtained by multiplying the total applied load by the distance to the face of the column or to the centerline of the column. The deflection measured at a distance of 42 in. (1067 mm) from the face of the column or 6 in. (152 mm) from the edge of the slab was referred to as the edge deflection. The moment at the face of the column versus the edge deflection is shown for all four specimens in Fig. 7. The moment, shear, and edge deflections at peak load for each specimen and the observed failure mode are tabulated in Tables 3 and 4.

The moment-deflection behavior for S1 was linear to the first cracking point. Thereafter, the stiffness of the slab decreased gradually to the point of yielding of the bonded steel. After yielding of the steel occurred, the stiffness of the slab decreased more rapidly. As the ultimate moment was approached, crushing began to develop at the intersection of the bottom surface of the slab and the east column face. Once crushing was fully developed, the capacity of the slab decreased with increasing edge displacement. The ultimate moment of 43.23 kips-ft (58.62 kN-m) was accompanied by an edge deflection of about 1.45 in. (36.8 mm). The maximum deflection achieved before the test was stopped was about 2.4 in. (61 mm), and the final residual deflection of the specimen at the conclusion of the test was 1.15 in. (29.2 mm). A photograph of S1 at completion of testing is shown in Fig. 8, the deflection profile is given in Fig. 9, and the crack pattern for the top surface is shown in Fig. 10.

It is apparent that considerable rotation occurred at the face of the column, and this made the largest contribution to the edge displacement. The slab folded down markedly along a yield line passing along the face of the column. The specimen was unloaded to zero load and then reloaded three times during the course of the test: just after cracking, just after yield, and just after the ultimate load. This cycling of the load had no visi-

Table 3 — Measured and calculated ultimate moment at face of column*

Specimen	Moment due to: Dead load of slab plus loading frame	Moment due to: Applied load	Measured moment	Calculated moment: ACI 318-77	Calculated moment: Based on measured internal forces	Mode of failure
S1	2.86	40.37	43.23	40.95	41.65	Flexure
S2	2.49	34.52	37.01	37.10	36.47	Shear
S3	2.49	27.30	29.79	27.90	29.29	Flexure
S4	2.25	24.14	26.39	24.68	26.09	Shear

*Shear in kips; moments in k-ft.
1 kip = 4.48 kN; 1 k-ft = 1.356 kN-m.

Table 4 — Ultimate shear and moment at centerline of columns*

Specimen	Shear due to: Dead load of slab plus loading frame	Shear due to: Applied load	Shear due to: Total load	Moment due to: Dead load of slab plus loading frame	Moment due to: Applied load	Moment due to: Total load	Deflection at edge of slab
S1	1.45	11.53	12.98	3.50	46.12	49.62	1.449
S2	1.45	17.26	18.71	3.12	43.15	46.27	0.919
S3	1.45	13.65	15.10	3.12	34.12	37.24	1.511
S4	1.45	24.14	25.59	2.87	36.21	39.08	0.837

*Shear in kips; moments in k-ft.
1 kip = 4.48 kN; 1 k-ft = 1.356 kN-m.

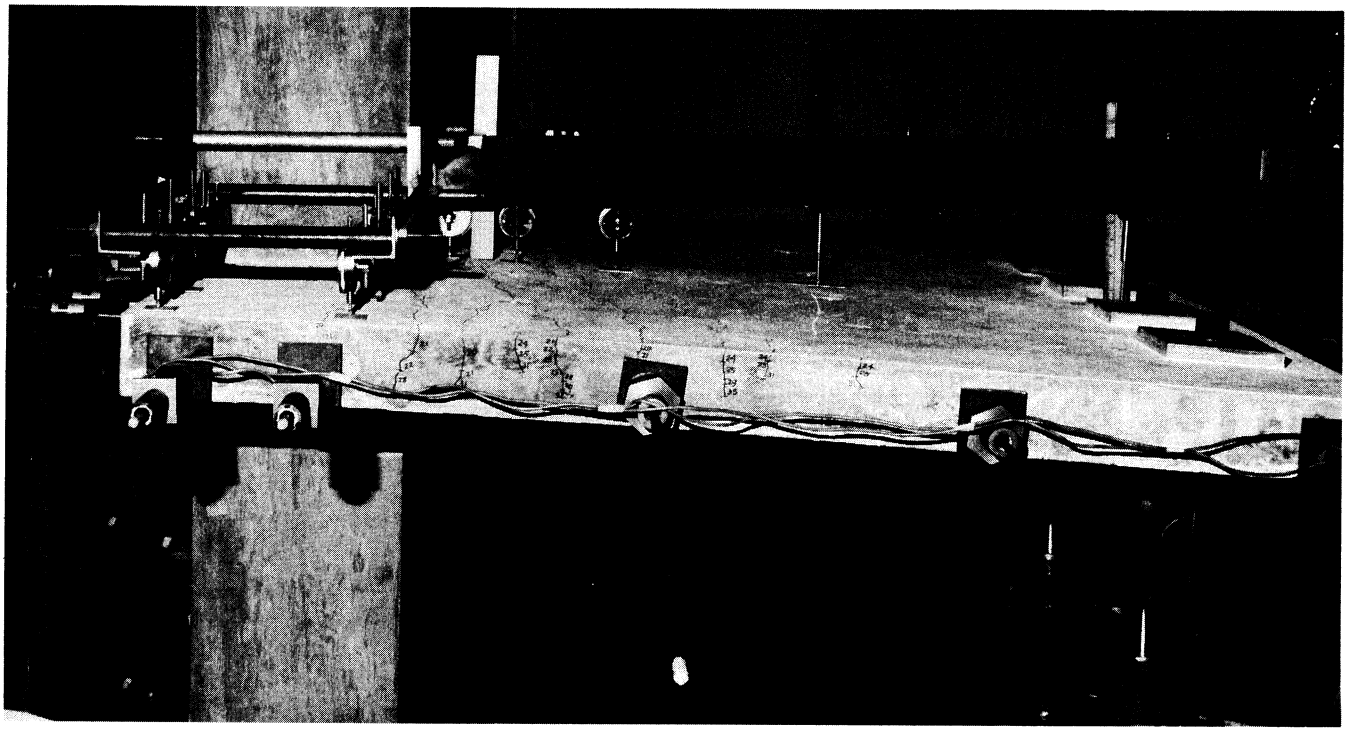

Fig. 8—Photo of Specimen S1 at completion of testing

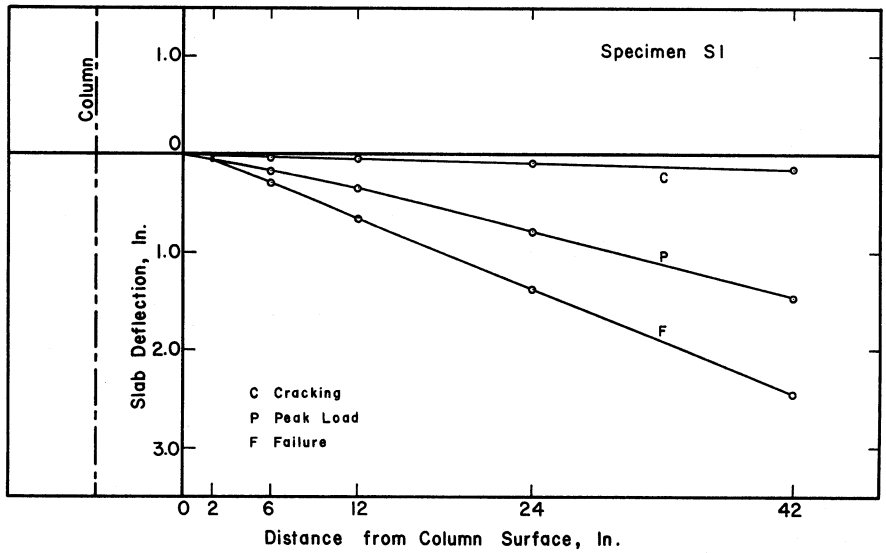

Fig. 9—Deflection profiles of Slab S1

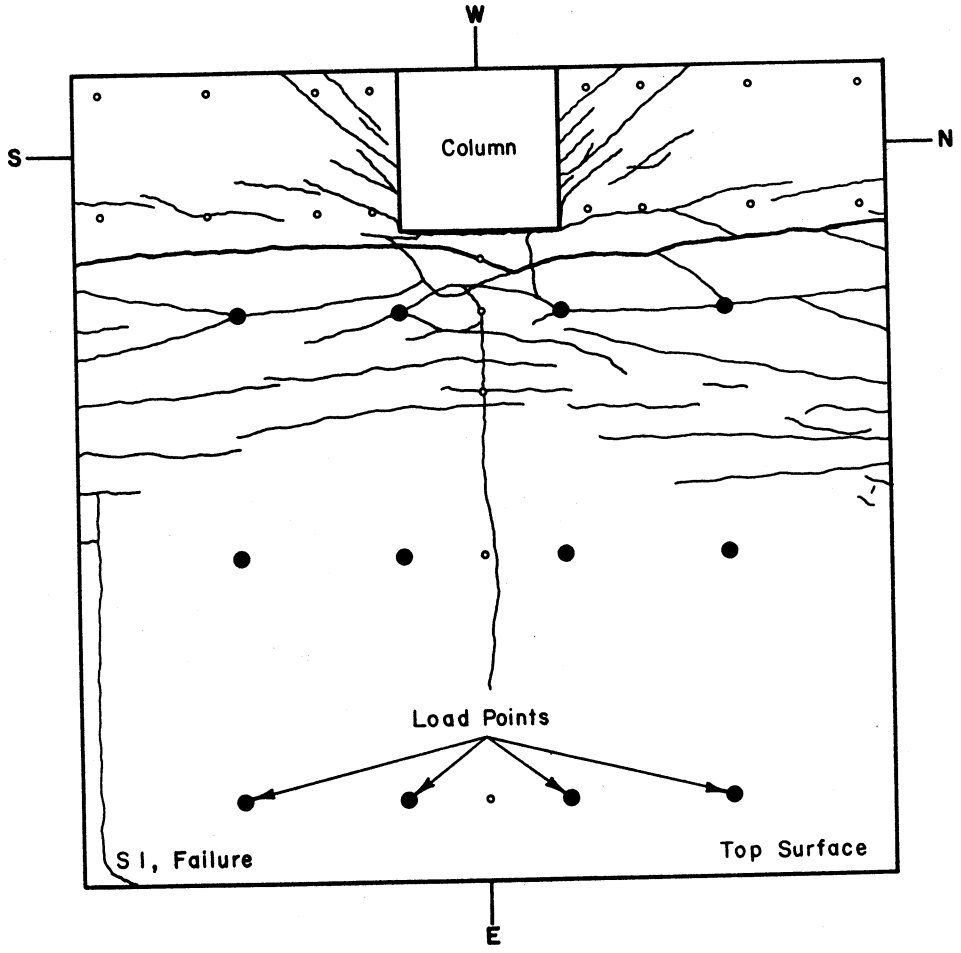

Fig. 10—Crack pattern at failure on the top surface of Specimen S1

ble effect on the response of the specimen. The measured behavior indicates that the specimen was quite ductile.

Specimen S2 was identical to S1 in the amounts and distribution of reinforcment, in geometry, and in column size. The variable was the location of the loading point which changed the moment-to-shear ratio. The moment-deflection behavior was essentially the same as for Specimen S1 during the early stages of loading. Small differences in response were observed due to slightly differing concrete strengths and prestressing forces. After yielding of the top bonded reinforcement, however, the responses of Specimens S1 and S2 differed considerably. Specimen S2 failed in shear in a rather brittle fashion with a sudden collapse of the compression zone. The slab failed along a surface formed by inclined cracks in the immediate vicinity of the column. The failure surface had a shape roughly approximating that of a truncated cone spreading from the column. As soon as shear failure occurred, the pressure in the hydraulic system relieved itself and the load decreased to about 1.8 kips (8.0 kN). Since details of S1 and S2 were identical, the moment capacities of the slabs should have been the same. However, the presence of the higher shear caused failure at a moment of 37.01 kips-ft (50.19 kN-m), which is considerably lower than the maximum achieved by S1. A photograph of the specimen is shown in Fig. 11, the crack pattern on the surface of the slab is shown in Fig. 12, and the deflection profile is given in Fig. 13.

Specimen S3 had a different reinforcement pattern than S1 or S2, since the banded tendons ran parallel to the free edge rather than perpendicular to it. This resulted in fewer tendons resisting the applied moment at the connection. Therefore, the moment capacity was 29.79 kips-ft (40.40 kN-m), which was considerably lower than for S1. The overall behavior was very similar to that of S1, and a ductile failure occurred in flexure along a yield line extending across the slab at the face of the column.

Specimen S4 was identical to S3 except for the point of loading. However, a brittle-type shear failure occurred in the specimen at a moment of only 26.39 kips-ft (35.78 kN-m). As with S2, the detrimental effect of high shear stresses on the ability of the slab to transmit moment was evident in the connection region.

The deflection profiles in Fig. 9 and 13 reveal the basic difference in the nature of the two types of failure: flexure and shear. As the failure load was approached for Specimens S1 and S3, considerable rotation occurred along the front face of the column, which resulted in a folding action of the slab. Due to the con-

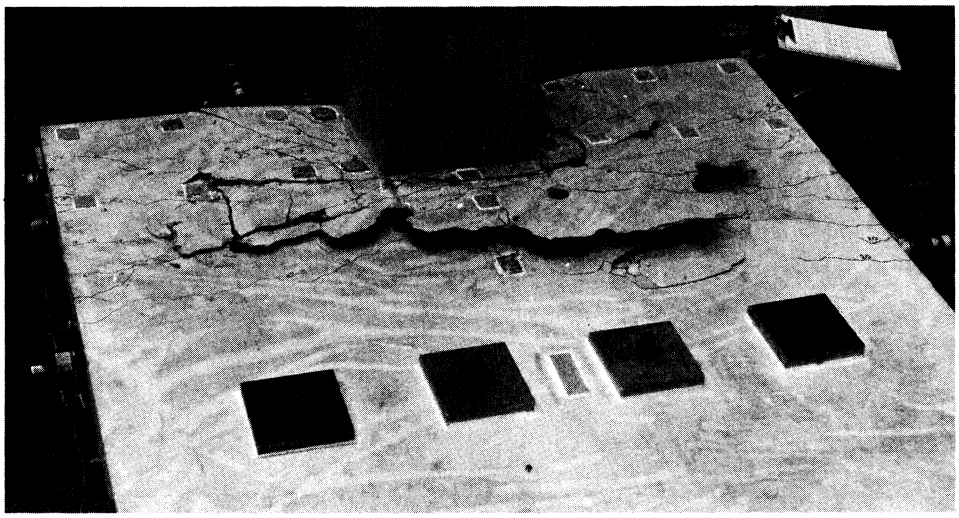

Fig. 11—Photo of Slab S2 at completion of testing

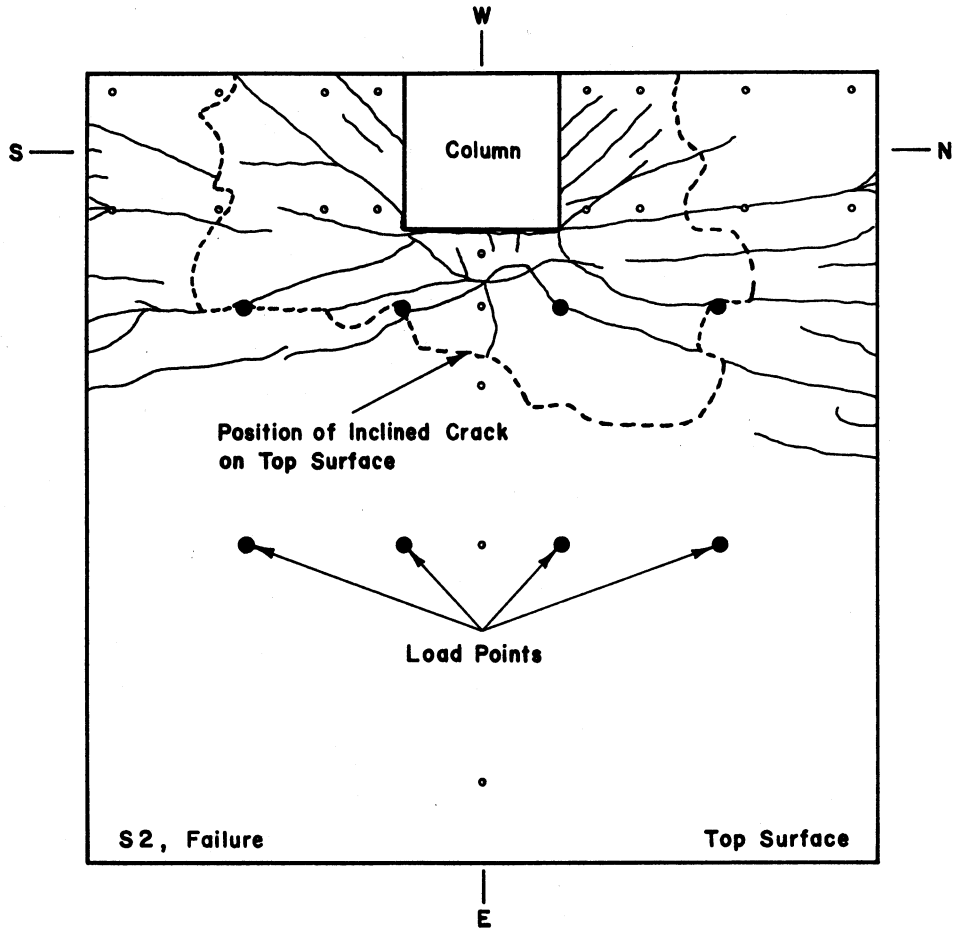

Fig. 12—Crack pattern at failure on the top surface of Specimen S2

centration of tendons through the column region, Specimens S1 and S2 were both stiffer and stronger than S3 and S4. This also produced some interesting differences in the failure mechanism between S2 and S4. The local failure of S2 was accompanied by significant crushing of the compression zone of the slab, while no similar crushing was observed for S4. The absence of bottom steel in the slab passing through the column, and the crushing of the compression zone were the main causes of significant movement of the slab down the column after shear failure had occurred. The top steel is not effective in providing postpunching resistance because it tends to tear out a substantial area of the concrete over the slab. Because of the lack of

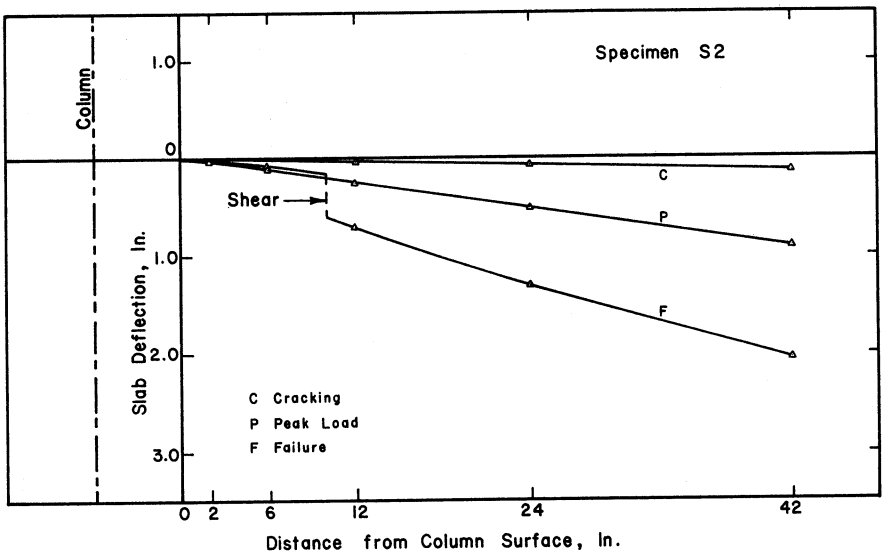

Fig. 13—Deflection profiles for Specimen S2

crushing, the failure region of S4 was not as pronounced as for S2.

Tendon stress

The tendon forces throughout the tests were measured with load cells. A plot of the nominal tendon stress versus moment for the tendon in each specimen that experienced the largest stress increase is shown in Fig. 14. This was always one of the tendons passing through the column and normal to the slab edge. The tendon stress increased gradually until yielding developed in the bonded bars, as has been observed before for members with unbonded tendons. As the applied load approached the failure load, larger increases in tendon stress were obtained at the expense of large deflections. As expected, very little change in stress occurred in the tendons in the transverse direction.

The tendon-stress increase versus moment relationship is highly nonlinear but is very similar to the moment versus deflection relationship of the specimens. Fig. 15 shows the relationship of tendon-force increase versus slab rotation for the same tendons as were shown in Fig. 14. The rotation at each load point was obtained by dividing the deflection of the slab at the loading point by the distance from that point to the face of the column. After yielding of the bonded steel, the relationship between tendon stress increase and rotation is essentially linear. This result is not unexpected, since it indicates that the tendon-stress increase is primarily a geometrical problem dependent on the initial geometry of the specimen and on the total rotation in the hinging region. The tendon stress increase is directly related to the total change in length of the slab at the level of the tendon. Note that the total increase in tendon stress was considerably smaller than that predicted by current design methods. Also, the increase in tendon stress for the two specimens that failed in shear was insignificant. These points will be discussed presently.

ANALYSIS OF TEST RESULTS

Flexural strength and tendon stresses

Table 3 lists the moments that were measured or calculated for the critical section at the face of the column, which is the appropriate section to consider the flexural strength using the yield line theory. The observed strengths equaled or exceeded the capacities predicted by the 1977 ACI Building Code provisions and the known material strengths. However, undue importance should not be placed on this comparison, because the strength was achieved in ways not anticipated in the code provisions. Furthermore, only Specimens S1 and S3 failed in flexure. The other two suffered flexural distress but failed in a shear mode.

The sections contained both post-tensioned unbonded tendons and bonded Grade 60 (414 MPa) No. 3 (9.5 mm) reinforcing bars, and both made significant contributions to the moment capacity. However, the stresses in the unbonded tendons were somewhat less than anticipated by the ACI Building Codes, and the stresses in the No. 3 deformed bars were larger than the yield stress in all cases and significantly greater in Specimens S1 and S3, because of strain hardening.

Table 5 lists stresses in the tendon that had the largest stress increase in each of the four specimens, along with the values computed using the 1977 and 1983 ACI Building Codes. In no case did the increase in tendon stress above the prestress level existing at the beginning of the test exceed half the increase expected following the 1977 ACI Building Code. Further, the greatest increase was just 84 percent of that predicted by the 1983 ACI Building Code. The change in the 1983 ACI Building Code that reduced the computed value of f_{ps} in shallow unbonded members was clearly a step in the right direction, but that particular problem cannot be presumed solved. The average stress increase across the width of the slab ranged from 65 to 81 percent of the maximum stress increase.

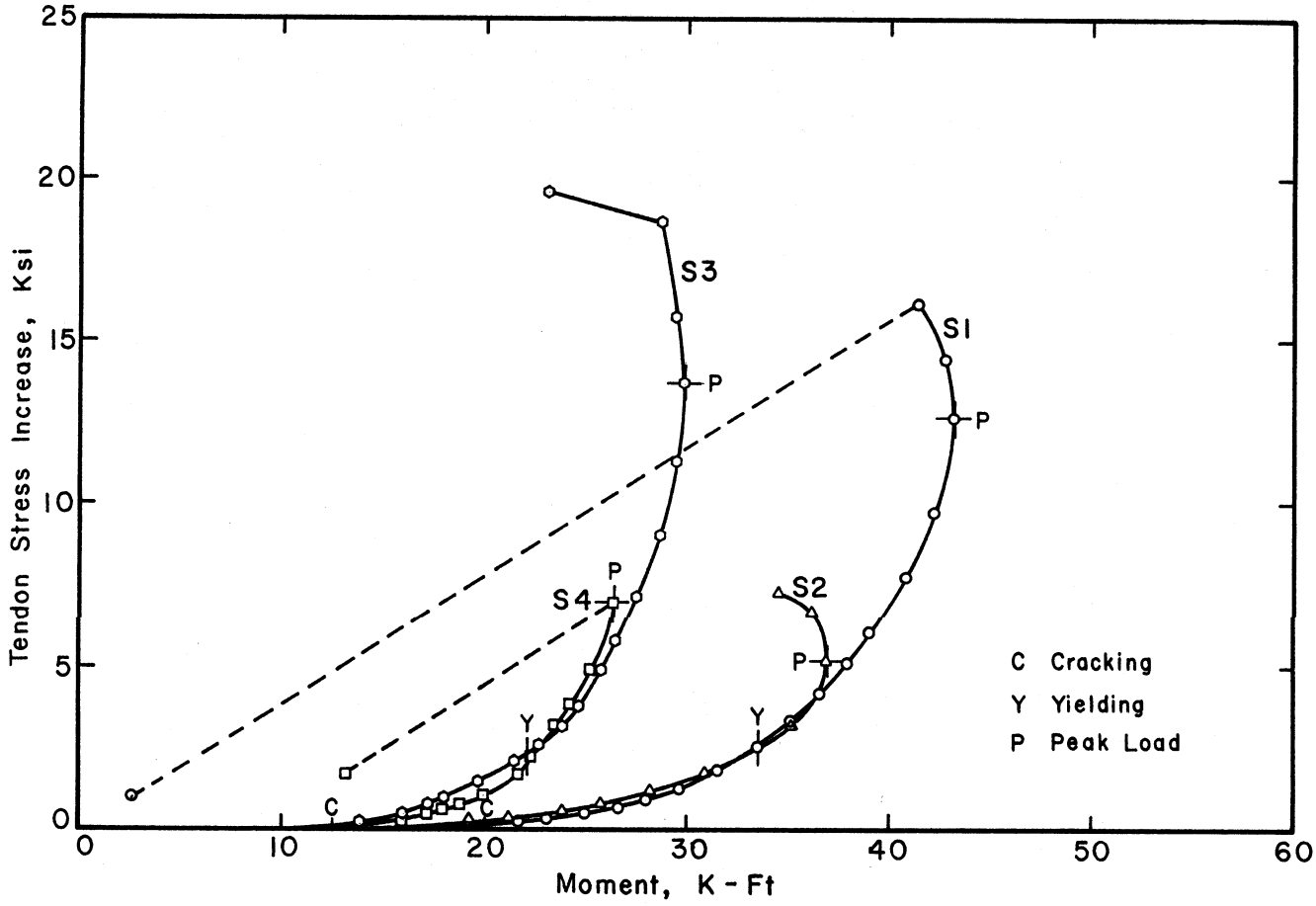

Fig. 14—Tendon stress increase versus moment for tendons passing through column

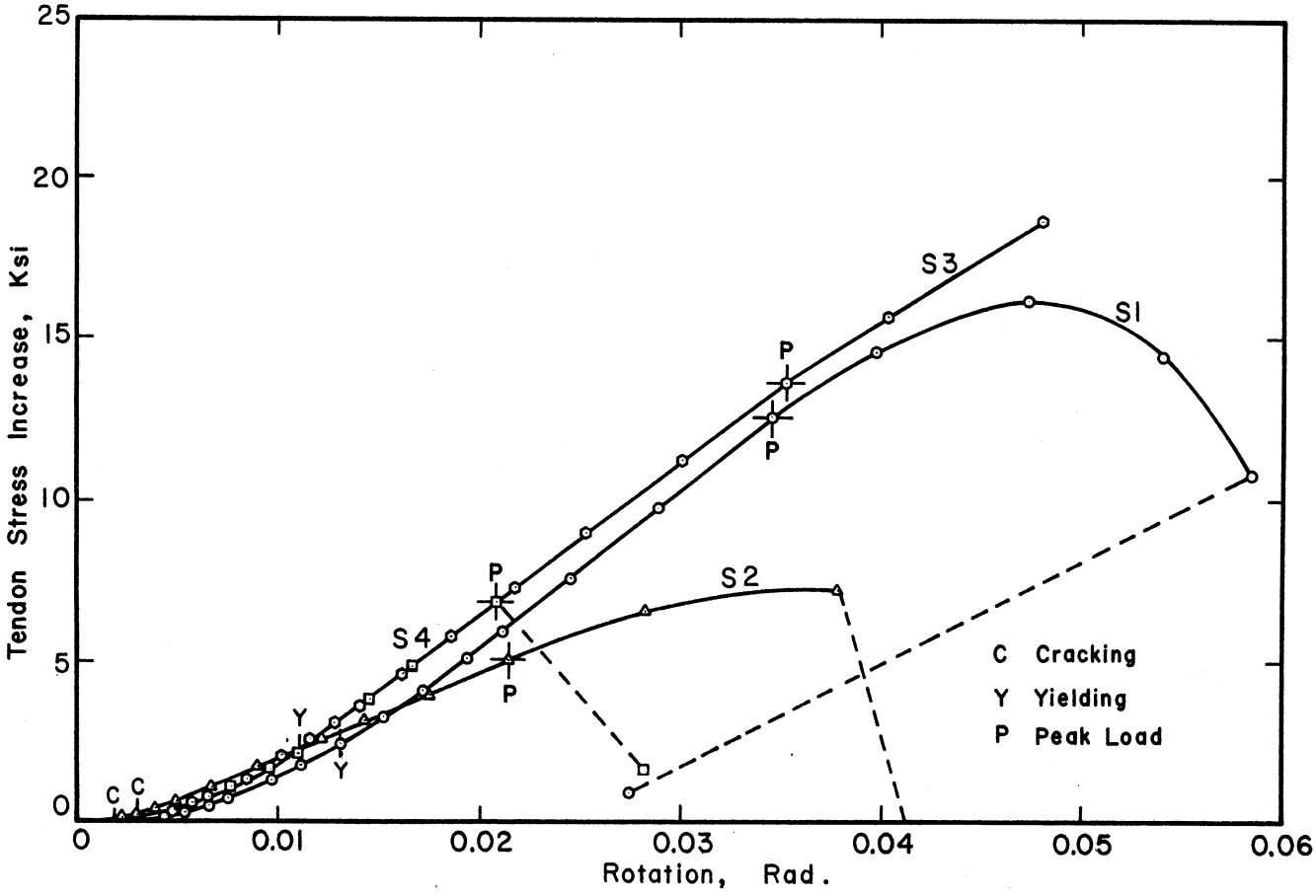

Fig. 15—Tendon stress increase versus rotation for tendons passing through column

Table 5 — Maximum increase in tendon stress, ksi*

Specimen	f_{se}	Increase in steel stress, δf_{ps}		
		Measured	ACI 318-77	ACI 318-83
S1	170.75	12.63	25.0	15.0
S2	182.02	5.20	22.7	14.2
S3	179.74	14.07	44.5	21.5
S4	188.61	6.99	48.9	23.0

*1 ksi = 6.895 MPa.

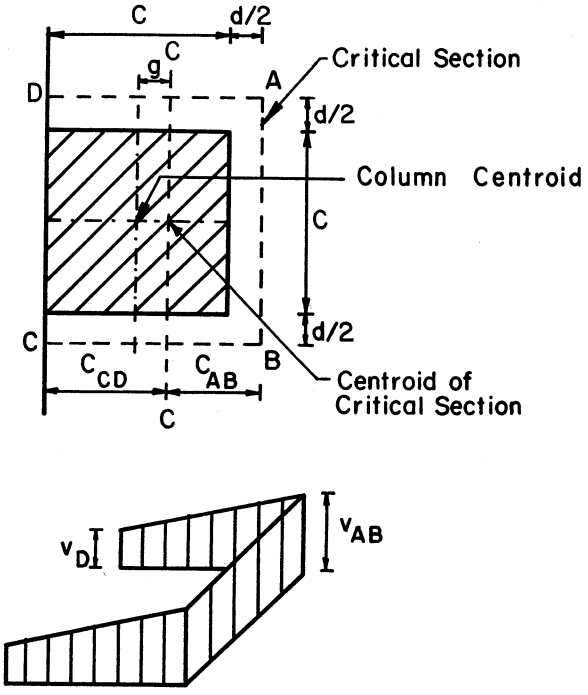

Fig. 16—Assumed distribution of shear stress for exterior column connections

The No. 3 (9.5 mm) reinforcing bars had a measured yield stress of 72.73 kips/in.^{2} (501 MPa). The yield plateau was relatively short, with strain hardening beginning at 0.005 strain. On the basis of strain measurements, the stresses in the No. 3 (9.5 mm) bars at the time of slab failure were found to be: S1, f_s = 83.3 kips/in.^{2} (574 MPa); S2, f_s = 75.2 kips/in.^{2} (519 MPa); S3, f_s = 90.8 kips/in.^{2} (626 MPa); and S4, f_s = 78.9 kips/in.^{2} (544 MPa). These stress values, plus the measured tendon forces, were used in the calculation of the moments based on measured internal forces that are listed in Table 3. The agreement between these calculated moments and the measured moments is quite good, and this seems to constitute an adequate explanation of the flexural equilibrium of the specimens. However, it is not a fully rational explanation because there is no adequate method for predicting the final stress in the unbonded tendons.

Shear strength

It has long been recognized that the shear strength of a slab-column connection cannot be considered independently of the flexural behavior. The ACI Building Codes are based on the computation of a maximum shear stress on a critical section located at a distance of $d/2$ away from the face of the column, as shown in Fig. 16. The stress criteria are given in Section 11.12 of ACI 318-83, and its Commentary[5] gives the appropriate equations. The basis for the equation is the assumption that there is a direct shear stress, in terms of force/area, plus a second component related to the unbalanced moment that must be transferred from the slab to the column. Part of the unbalanced moment is transferred directly by bending of the slab at Face AB of Fig. 16, and the rest is transferred by shear stresses which are nonuniformly distributed around the shear perimeter.

The equation for the maximum shear stress is an elastic equation, and the equation leading to the fraction of the slab moment that must be transmitted by shear stresses is an empirical equation based on a relatively limited amount of data for reinforced concrete (not prestressed) slabs. The ACI Building Code endorses the use of these equations for prestressed slabs, but with a number of specific limits. One of the objectives of this test series was to explore these limits.

For reinforced concrete slabs supported on square columns, the limiting shear stress is

$$v_c = 4\sqrt{f'_c}\ \text{lb/in.}^2 \quad (1)$$
$$= \sqrt{f'_c}/3\ \text{MPa} \quad (1a)$$

This stress limit is retained for prestressed concrete slabs and for exterior columns. For interior columns, the limiting shear stress becomes

$$v_u = 3.5\sqrt{f'_c} + 0.3 f_{pc} + V_p/b_o d\ \text{lb/in.}^2 \quad (2)$$
$$= 0.3\sqrt{f'_c} + 0.3 f_{pc} + V_p/b_o d\ \text{MPa} \quad (2a)$$

There are additional restrictions on this equation, because of lack of test data outside this range of variables

$$f'_c \leqslant 5000\ \text{lb/in.}^2\ (\leqslant 34.5\ \text{MPa})$$
$$125 \leqslant f_{pc} \leqslant 500\ \text{lb/in.}^2\ (0.86 \leqslant f_{pc} \leqslant 3.45\ \text{MPa})$$

The equations for shear stress were derived for use with moments relative to the centroid of the column, rather than relative to the face of the column. The measured moments from the tests, with respect to the column centroid, are given in Table 4, as are the failure shear forces. The moments are larger than those given in Table 3 because of the different reference section, but they are consistent.

Table 6 contains comparisons between measured and computed strengths, where the computed values were based on the two ACI Building Code shear-stress values cited previously. It is clear that there is a significant bonus in the predicted strength if the effect of the prestress f_{pc} can be taken into account. The predicted strengths were computed using the measured f'_c values, and with f_{pc} taken as the stress perpendicular to the free end of the slab. The f_{pc} values are listed in Table 2, and are for the west-east direction. The different pre-

compression parallel to the edge of the slab was not taken into account.

The use of the relatively high values of f_{pc} for Specimens S1 and S2 has been questioned in some earlier oral discussion of these test results, on the basis that the average f_{pc} over the full width of a panel is much smaller. However, the authors feel that these values are appropriate, since the local stress distribution at sections near the edge of the slab must be closely related to the actual local strand spacing. If an interior column were being considered, the value of f_{pc} averaged over a full-panel width would clearly be appropriate, but the edge column case is different.

It is also clear that the measured strengths were greater than the predicted strengths, by various margins. The best agreement between the computed strength, using the shear stress from Eq. (2), and the measured strength was for Specimen S2, which failed in shear. For S2, the ratio of V_{test}/V_{calc} was 1.03. The ratio was about 1.12 for S3 and S4, and 1.23 for S1. None of these is excessive, relative to the scatter often found in shear strength test data.

There remain some troubling aspects of the behavior and predicted strengths of these slab specimens. All reached or exceeded the moment capacity predicted on the basis of the 1977 ACI Building Code. Predicted values of M_n in accordance with the 1983 ACI Building Code would be somewhat smaller. However, the flexural capacities were reached because of the importance of strain hardening of the bonded No. 3 bar reinforcement. The stresses in the unbonded tendons were smaller than the ACI Building Code predictions, and the increase in stress beyond the initial prestress value was much smaller than anticipated in Specimens S2 and S4, which failed in shear.

The specimens also reached loads larger than the predicted shear-failure load. Yet two failed in shear and two in flexure. The current ACI Building Code criteria do not appear to give a reliable way to tell which of these slabs should have been expected to fail in flexure, and which to fail in shear.

The most promising alternatives to the ACI Building Code's shear-stress approach seem to be beam analogies, in which the slab is replaced by pseudobeams framing into each face of the column. These will not be discussed here, but analysis methods suggested by Islam and Park[6] and Hawkins and Corley[7] are applied to these specimens in Reference 3.

CONCLUSIONS AND RECOMMENDATIONS

The results of this limited series of tests support the use of the shear stress from Eq. (2), which includes a contribution from the prestress in the concrete f_{pc}. All specimens resisted larger forces than predicted on the basis of this limiting shear stress.

The 1983 ACI Building Code limitations on maximum values of concrete strength f'_c and precompression f_{pc} do not appear to be necessary on the basis of these tests. All concrete was significantly stronger than f'_c = 5000 lb/in.^{2} (34.5 MPa), and f_{pc} was significantly greater than 500 lb/in.^{2} (3.45 MPa) in two of the specimens.

Table 6 — Comparison of measured and predicted shear strength using ACI model

	Predicted shear strength*				Measured strength		
	$v_{cw} = 3.5\sqrt{f'_c} + 0.3f_{pc}$		$v_c = 4\sqrt{f'_c}$				Mode of failure
Specimen	V_u†	M_u‡	V_u	M_u	V_u	M_u	
S1	10.58	40.02	7.76	28.74	12.98	49.62	Flexure
S2	18.17	44.93	12.38	30.45	18.71	46.27	Shear
S3	13.47	33.17	12.13	29.83	15.10	37.24	Flexure
S4	22.80	34.90	20.68	31.72	25.59	39.08	Shear

*Based on measured f'_c values and on f_{pc} perpendicular to free edge.
†Ultimate shear V_u in kips.
‡Ultimate moment M_u in k-ft.
1 kip = 4.448 kN; 1 k-ft = 1.356 kN-m.

All experimental reports conventionally end with a recommendation that more tests are needed. This is no exception. Only one earlier test of a pretensioned slab-edge column connection is known,[8] and five tests hardly justify sweeping changes in the current design procedures, even when the results are favorable and fairly consistent. Other tests, with different material strengths, geometries, and boundary conditions are needed to lend credence to empirical approaches to the problem, and to yield additional hard facts to researchers who are trying to employ different rational or semi-rational approaches.

REFERENCES

1. ACI Committee 318, "Building Code Requirements for Reinforced Concrete (ACI 318-77)," American Concrete Institute, Detroit, 1977, 102 pp.

2. ACI Committee 318, "Building Code Requirements for Reinforced Concrete (ACI 318-83)," American Concrete Institute, Detroit, 1983, 111 pp.

3. Sunidja, H.; Foutch, D. A.; and Gamble, W. L., "Response of Prestressed Concrete Plate-Edge Column Connections," Civil Engineering Studies, *Structural Research Series* No. 498, University of Illinois, Urbana, Mar. 1982, 232 pp.

4. ACI-ASCE Committee 423, "Tentative Recommendations for Prestressed Concrete Flat Plates," ACI JOURNAL, *Proceedings*, V. 71, No. 2, Feb. 1974, pp. 61-71.

5. ACI Committee 318, "Commentary on Building Code Requirements for Reinforced Concrete (ACI 318-83)," American Concrete Institute, Detroit, 1983, 155 pp.

6. Islam, Shafiqul, and Park, Robert, "Tests on Slab-Column Connections with Shear and Unbalanced Flexure," *Proceedings*, ASCE, V. 102, ST3, Mar. 1976, pp. 549-568.

7. Hawkins, N. M., and Corley, W. G., "Transfer of Unbalanced Moment and Shear from Flat Plates to Columns," *Cracking, Deflection, and Ultimate Load of Concrete Slab Systems*, SP-30, American Concrete Institute, Detroit, 1971, pp. 147-176.

8. Trongtham, N., and Hawkins, N. M.,"Moment Transfer to Columns in Unbonded Post-Tensioned Prestressed Concrete Slabs,"*Report* No. SM 77-3, Department of Civil Engineering, University of Washington, Seattle, Oct. 1977, 204 pp.